DOI: 10.1002/ejic.201000560

Synthesis, Properties, and Redox Behavior of Ferrocene-Substituted Bis(3-methylthio-1-azulenyl)methylium Ions

Taku Shoji,*[a] Junya Higashi,[b] Shunji Ito,[c] and Noboru Morita[b]

Keywords: Azulene / Ferrocene / Carbocations / Cyclic voltammetry / Electrochemistry

Novel ferrocene-substituted bis(3-methylthio-1-azulenyl)-methylium ions **5**$^+$ and **6**$^+$ were synthesized by the hydride abstraction reaction of the corresponding hydro derivatives **3** and **4** with 2,3-dichloro-5,6-dicyano-1,4-benzoquinone (DDQ). Compounds **3** and **4** were readily prepared by the acid-catalyzed condensation reaction of 1-methylthioazulenes **1** and **2** with ferrocenecarbaldehyde. The redox behavior of **5**$^+$ and **6**$^+$ was examined by cyclic voltammetry (CV) and differential pulse voltammetry (DPV), which revealed their amphoteric multistep redox properties. Moreover, these cations exhibited a significant color change under electrochemical reduction conditions, which was revealed by visible spectroscopy.

Introduction

Ferrocene has attracted much interest due to its facile oxidation properties with a lower potential to form a stabilized radical cation (ferrocenium ion). Thus, a large number of compounds incorporating ferrocenyl groups have been synthesized, and their properties based on the intramolecular interactions with the ferrocenyl groups have been extensively studied.[1]

Azulene ($C_{10}H_8$) has attracted the interest of many research groups owing to its unusual properties as well as its blue color.[2] Recently, Nielsen et al. reported efficient synthesis by a novel route of functionalized azulenes from dihydroazulene precursors. They also concluded that these new azulene derivatives can be applied in molecular electronics using their photochemical properties.[3] We have reported the synthesis of various redox-active chromophores incorporated with azulene substituents aimed for the creation of stabilized electrochromic materials.[4] As a part of this study, we have also reported the synthesis of bis(1-azulenyl)ferrocenylmethylium hexafluorophosphates with high thermodynamic stabilities by the hydride abstraction reaction of the corresponding hydrocarbon derivatives.[5] These salts exhibited reversible oxidation and reduction waves in cyclic voltammetry (CV) and significant color changes under electrochemical reduction conditions.

In 2000, Bryce et al. reported the synthesis of a multistage redox system conjugated with ferrocene and tetrathiafulvalene (TTF) binding with methylthio moieties.[6] Recently, we have reported a facile and efficient synthetic route to several 1-azulenylmethyl and phenyl sulfides and 1,3-bis(methylthio)- and 1,3-bis(phenylthio)azulenes via 1-azulenylsulfonium and 1,3-azulenediyldisulfonium ions.[7] We have revealed that these 1-azulenyl sulfides exhibit a reversible reduction wave in CV.[7,8] Thus, similar with methylthio-substituted TTF derivatives, ferrocene-substituted bis(3-methylthio-1-azulenyl)methylium ions should provide stable and amphoteric redox behavior under the electrochemical reaction conditions. In this paper, we report the synthesis and properties of ferrocenylbis(3-methylthio-1-azulenyl)methylium salts **5**$^+\cdot PF_6^-$ and **6**$^+\cdot PF_6^-$, in particular, their redox behavior examined by CV and differential pulse voltammetry (DPV). The electrochromic behavior of cations **5**$^+$ and **6**$^+$ was also examined. They display distinct changes in their absorption spectra in different oxidation states.

Results and Discussion

Synthesis

1-Methylthioazulene derivatives **1** and **2** were prepared according to the procedure reported by us recently.[7] The synthesis of **5**$^+\cdot PF_6^-$ and **6**$^+\cdot PF_6^-$ was accomplished by hydride abstraction from the corresponding methane derivatives, according to our previous report.[5] The reaction of 1-methylthioazulene (**1**) and 1-methylthio-6-*tert*-butylazulene (**2**) with ferrocenecarboxaldehyde in acetic acid at 50 °C for 24 h afforded **3** and **4** in 69% and 91% yields, respectively

---

[a] Department of Chemistry, Faculty School of Science,
Shinshu University,
Matsumoto 390-8621, Japan
Fax: +81-263-37-2476
E-mail: tshoji@shinshu-u.ac.jp
[b] Department of Chemistry, Graduate School of Science,
Tohoku University,
Sendai 980-8578, Japan
[c] Graduate School of Science and Technology,
Hirosaki University,
Hirosaki 036-8561, Japan

Supporting information for this article is available on the WWW under http://dx.doi.org/10.1002/ejic.201000560.

(Scheme 1). Yields for the reaction of **2** with the aldehyde is relatively high compared with that of **1**. These results suggest that the *tert*-butyl group on the azulene ring at the 6-position enhances the reactivity toward the aldehyde.

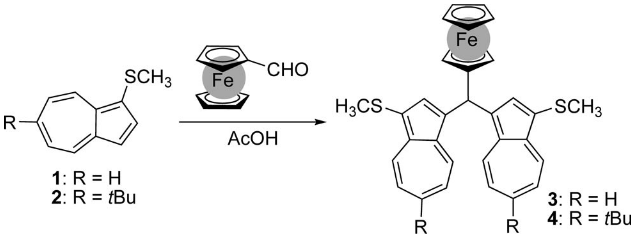

Scheme 1.

Salts **5**$^{+}\cdot$PF$_6^-$ and **6**$^{+}\cdot$PF$_6^-$ were synthesized by the hydride abstraction reaction of the corresponding hydro derivatives **3** and **4**. The reaction of **3** with 2,3-dichloro-5,6-dicyano-1,4-benzoquinone (DDQ) in dichloromethane at room temperature followed by the addition of a 60% aqueous HPF$_6$ solution yielded the expected cation **5**$^+$ as a hexafluorophosphate salt in 96% yield (Scheme 2). Likewise, the oxidation of **4** with DDQ, followed by the addition of HPF6 solution, afforded the corresponding hexafluorophosphate **6**$^{+}\cdot$PF$_6^-$ in 93% yield. These new salts, **5**$^{+}\cdot$PF$_6^-$ and **6**$^{+}\cdot$PF$_6^-$, were stable, deep-colored crystals and are storable in the crystalline state.

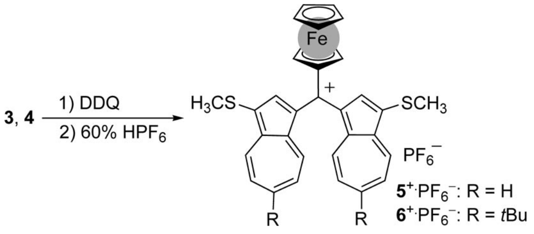

Scheme 2.

Spectroscopic Properties

Compounds **3**, **4**, **5**$^{+}\cdot$PF$_6^-$, and **6**$^{+}\cdot$PF$_6^-$ were fully characterized by spectroscopic data, which are presented in the Experimental Section. The mass spectra of **3** and **4** showed the correct molecular ion peaks. The high-resolution mass spectrum of salts **5**$^{+}\cdot$PF$_6^-$ and **6**$^{+}\cdot$PF$_6^-$ ionized by ESI showed the correct [M – PF$_6$]$^+$ ion peaks, which indicates the ionic structure of these salts. The characteristic stretching vibration bands of the hexafluorophosphate group in salts **5**$^{+}\cdot$PF$_6^-$ and **6**$^{+}\cdot$PF$_6^-$ were observed at 838–839 (strong) and 557 (medium) cm^{-1} in their IR spectra. These results are consistent with the structure of these products.

The UV/Vis spectra of **5**$^{+}\cdot$PF$_6^-$ and **6**$^{+}\cdot$PF$_6^-$ in acetonitrile are shown in Figure 1. The absorption maxima and extinction coefficients [log ε] of compounds **3**, **4**, **5**$^{+}\cdot$PF$_6^-$, and **6**$^{+}\cdot$PF$_6^-$, together with those of **7**$^{+}\cdot$PF$_6^-$ to **10**$^{+}\cdot$PF$_6^-$ (Figure 2), are summarized in Table 1. Compounds **3** and **4** showed characteristic absorptions in the visible region arising from the azulene system centered at 617 and 606 nm, respectively, in dichloromethane. The UV/Vis spectrum of **5**$^{+}\cdot$PF$_6^-$ and **6**$^{+}\cdot$PF$_6^-$ in acetonitrile displayed strong absorption in the visible region that extended up to the infrared region (**5**$^{+}\cdot$PF$_6^-$: 742 nm, **6**$^{+}\cdot$PF$_6^-$: 738 nm). The strong absorption of **5**$^{+}\cdot$PF$_6^-$ and **6**$^{+}\cdot$PF$_6^-$ in the visible region could be explained by the charge transfer (CT) transition between the two-substituted 3-methylthio-1-azulenyl moieties, as described by the resonance structure in Scheme 3. The longest wavelength absorption of compounds **5**$^{+}\cdot$PF$_6^-$ and **6**$^{+}\cdot$PF$_6^-$ exhibited a bathochromic shift compared with those of **7**$^{+}\cdot$PF$_6^-$ to **10**$^{+}\cdot$PF$_6^-$.

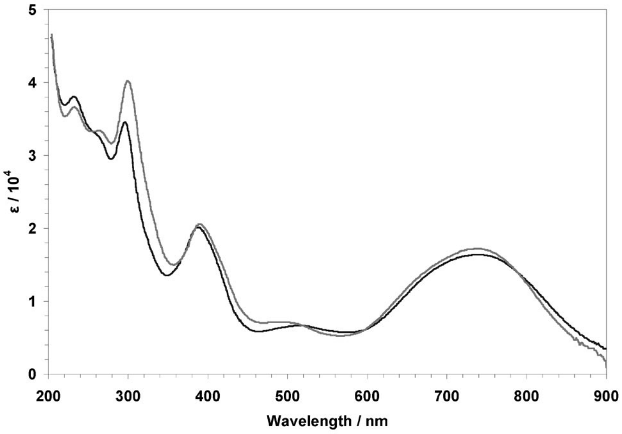

Figure 1. UV/Vis spectra of **5**$^{+}\cdot$PF$_6^-$ (black line) and **6**$^{+}\cdot$PF$_6^-$ (gray line) in acetonitrile.

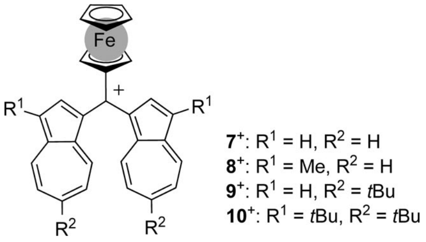

Figure 2. Bis(1-azulenyl)ferrocenylmethylium hexafluorophosphates **7**$^{+}\cdot$PF$_6^-$ to **10**$^{+}\cdot$PF$_6^-$.

Table 1. Absorption maxima and the corresponding absorption coefficients for **3**, **4**, **5**$^{+}\cdot$PF$_6^-$, and **6**$^{+}\cdot$PF$_6^-$, together with those of **7**$^{+}\cdot$PF$_6^-$ to **10**$^{+}\cdot$PF$_6^-$.

Sample	λ_{max} /nm [log ε]
3[a]	617 [2.77], 652 sh [2.76]
4[a]	606 [2.81]
5$^+$[b]	391 [4.31], 516 [3.83], 742 [4.21]
6$^+$[b]	391 [4.31], 493 [3.85], 738 [4.24]
7$^+$[b,c]	395 sh [4.15], 447 sh [4.14], 467 [4.16], 591 sh [4.10], 621 [4.20], 746 [3.84]
8$^+$[b,c]	468 sh [3.89], 497 [3.96], 629 sh [4.18], 655 [4.23], 711 sh [4.09]
9$^+$[a,d]	400 [4.41], 471 [4.08], 629 [4.29], 722 sh [3.95]
10$^+$[b,c]	461 sh [4.00], 486 [4.03], 657 [4.31], 693 sh [4.28]

[a] UV/Vis spectra were recorded in dichloromethane. [b] UV/Vis spectra were recorded in acetonitrile. [c] See ref.[5]. [d] See ref.[8]

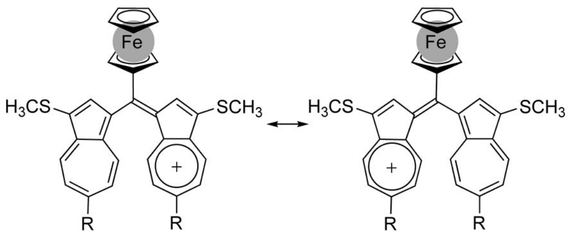

Scheme 3. Presumed intramolecular CT in cations **5**$^+$ and **6**$^+$.

The solvent dependence of the longest absorption maxima and the corresponding absorption coefficients (log ε) are summarized in Table 2. The UV/Vis spectra of **5**$^+$·PF_6^- and **6**$^+$·PF_6^- in different solvents are shown in the Supporting Information.

Table 2. Solvatochromic data for the longest wavelength absorption of **5**$^+$·PF_6^- and **6**$^+$·PF^-.

Solvent	**5**$^+$·PF_6^-	**6**$^+$·PF_6^-
	λ_{max} /nm [log ε]	λ_{max} /nm [log ε]
CH_2Cl_2	696 [4.13]	739 [3.98]
MeOH[a]	698 [4.05]	726 [3.89]
AcOEt[a]	696 [4.11]	724 [3.93]
Hexane[a]	697 [4.11]	714 [3.94]

[a] Dichloromethane (10%) was used to keep the compounds soluble.

The longest absorption maxima of **5**$^+$·PF_6^- in each solvent examined showed hypsochromic shifts compared with that in acetonitrile. Solvatochromism was also observed in the UV/Vis spectra of **6**$^+$·PF_6^-. Compound **6**$^+$·PF_6^- exhibited a CT absorption at λ_{max} = 739 nm in CH_2Cl_2, which was nearly equal to that in acetonitrile. When the solvent was changed from CH_2Cl_2 to hexane, **6**$^+$·PF_6^- exhibited a bathochromic shift by 25 nm in its CT absorption. These solvent dependences indicate the remarkable contribution of the intramolecular CT to the resonance hybrid for the excited state in addition to the ground state of **5**$^+$·PF_6^- and **6**$^+$·PF_6^-.

Redox Potentials

To clarify the electrochemical properties, the redox behavior of **3**, **4**, **5**$^+$·PF_6^-, and **6**$^+$·PF_6^- was examined by CV and DPV. Measurements were carried out with a standard three-electrode configuration. Tetraethylammonium perchlorate (0.1 M) in benzonitrile was used as a supporting electrolyte with platinum wire auxiliary and working electrodes. All measurements were carried out under an argon atmosphere, and potentials were related to an Ag/Ag$^+$ reference electrode and Fc/Fc$^+$ as an internal reference, which discharges at +0.15 V. The redox potentials (in volts vs. Ag/$AgNO_3$) of **3**, **4**, **5**$^+$·PF_6^-, and **6**$^+$·PF_6^-, together with those of **7**$^+$·PF_6^- to **10**$^+$·PF_6^-, are summarized in Table 3. The cyclic voltammograms of **3** and **5**$^+$·PF_6^- are shown in Figures 3 and 4, respectively.

Table 3. Redox potentials[a] of **3**, **4**, and **5**$^+$·PF_6^- to **10**$^+$·PF_6^-.

Sample	Method	E_1^{red} /V	E_1^{ox} /V	E_2^{ox} /V	E_3^{ox} /V
3	CV	–	+0.12	+0.41	+0.53
	(DPV)	(–1.84)	(+0.10)	(+0.39)	(+0.51)
4	CV	–	+0.12	+0.36	+0.49
	(DPV)	(–1.93)	(+0.10)	(+0.34)	(+0.47)
5$^+$	CV	–	+0.47	–	–
	(DPV)	(–0.69)	(+0.45)	–	–
6$^+$	(DPV)	(–0.74)	(+0.44)	(+0.64)	–
7$^{+[b]}$	CV	–0.76	+0.47	(+1.08)	–
8$^{+[b]}$	CV	–0.79	+0.43	(+0.95)	–
9$^{+[c]}$	CV	–0.82	+0.48	–	–
	(DPV)	(–0.80)	(+0.46)	(+1.02)	–
10$^{+[b]}$	CV	–0.87	+0.42	(+0.95)	–

[a] Redox potentials were measured by CV and DPV [V vs. Ag/$AgNO_3$, 1 mM in benzonitrile containing Et_4NClO_4 (0.1 M), Pt electrode (i. d.: 1.6 mm), scan rate = 100 mVs^{-1}, and Fc/Fc$^+$ = +0.15 V]. In the case of reversible waves, redox potentials measured by CV are presented. The peak potentials measured by DPV are shown in parentheses. [b] Redox potentials measured in acetonitrile. [c] See ref.[9]

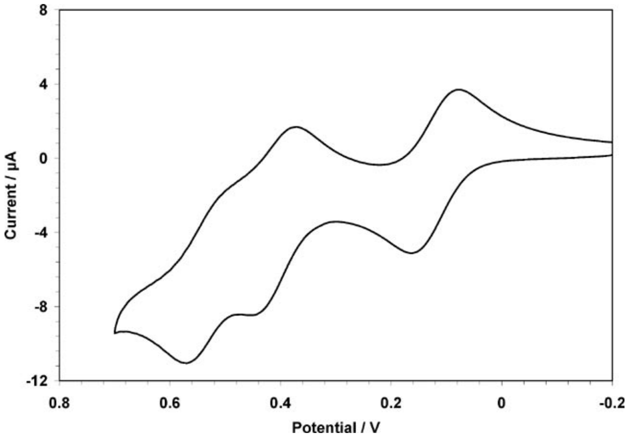

Figure 3. Cyclic voltammograms of the oxidation of **3** (1 mM) in benzonitrile containing Et_4NClO_4 (0.1 M) as a supporting electrolyte; scan rate 100 mVs^{-1}.

Electrochemical reduction of **3** showed an irreversible wave in CV, attributable to the generation of an unstable radical anion by the reduction of sulfur-substituted azulene moieties of **3**. The reduction potential was determined by DPV to be –1.84 V. The electrochemical oxidation of **3** exhibited a reversible three-step oxidation wave, whose potentials were identified as +0.10 V, +0.39 V, and +0.51 V by DPV, which might be attributed to the oxidation of ferrocene and two sulfur-substituted azulene rings, respectively (Figure 3). The first oxidation potential of **3** is slightly less positive than that of the parent ferrocene (+0.15 V), which is attributable to the electron-donating nature of the methine moiety substituted by the two azulene rings. The electrochemical reduction of **4** also exhibited an irreversible wave, which is attributable to the reduction of the sulfur-substituted azulene rings of **4** in CV. The reduction potential of **4** was relatively more negative than that of **3**. These results indicate that the *tert*-butyl group at the 6-position increases the persistence of the radical anion. Reversible three-stage

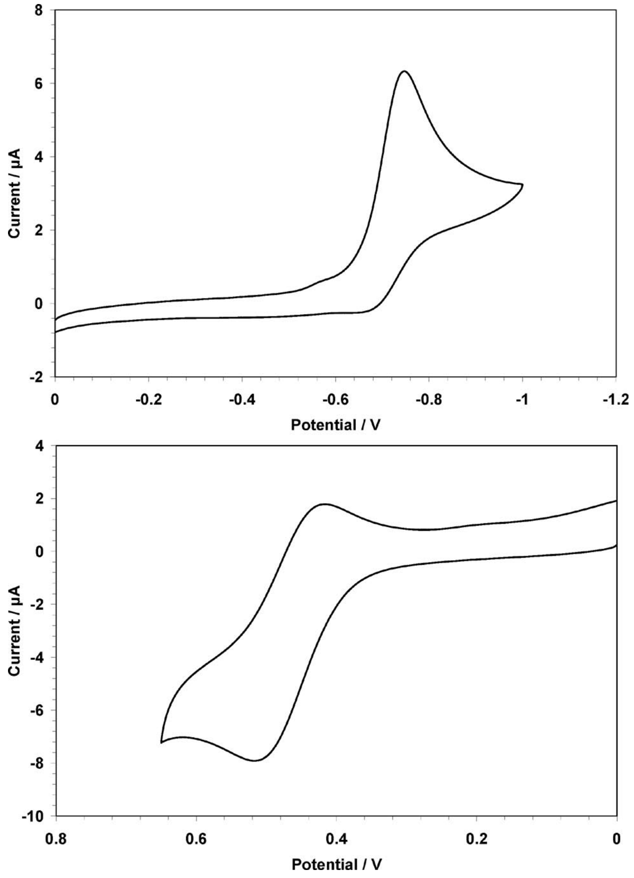

Figure 4. Cyclic voltammograms of reduction (upper) and oxidation (bottom) of $5^{+}\cdot PF_6^{-}$ (1 mM) in benzonitrile containing Et_4NClO_4 (0.1 M) as a supporting electrolyte; scan rate 100 mVs^{-1}.

oxidation waves were also observed for **4** in CV, which were identified as +0.10 V, +0.36 V, and +0.47 V by DPV.

The cyclic voltammograms for the reduction and the oxidation of $\mathbf{5}^{+}\cdot PF_6^{-}$ are shown in Figure 4. The electrochemical reduction of $\mathbf{5}^{+}\cdot PF_6^{-}$ showed an irreversible wave at –0.69 V in DPV due to the formation of a neutral radical species. The first reduction potential of $\mathbf{5}^{+}\cdot PF_6^{-}$ is slightly less negative than those of $\mathbf{7}^{+}\cdot PF_6^{-}$ to $\mathbf{10}^{+}\cdot PF_6^{-}$. This might be attributable to the methylthio substituents at the 3-positions of the azulene rings, which destabilize the cationic state by their electron-withdrawing nature, although the solvent for the measurements was different in these cases. The electrochemical oxidation of $\mathbf{5}^{+}\cdot PF_6^{-}$ showed a reversible wave at +0.47 V. This clearly indicates the generation of a cationic species by the oxidation of the ferrocene moiety of $\mathbf{5}^{+}\cdot PF_6^{-}$. The first oxidation potential of $\mathbf{5}^{+}\cdot PF_6^{-}$ is more positive than that of the parent ferrocene by +0.15 V under these conditions. These results are attributable to the reduction of the π-donating ability of ferrocene by the connection of the cation part in $\mathbf{5}^{+}\cdot PF_6^{-}$, that is, the lower HOMO level. Electrochemical reduction of $\mathbf{6}^{+}\cdot PF_6^{-}$ also exhibited an irreversible wave in CV, which indicates the formation of an unstable neutral radical species. Electrochemical oxidation of $\mathbf{6}^{+}\cdot PF_6^{-}$ also showed an irreversible oxidation wave at +0.44 V due to the generation of a cationic species. The first reduction potential of $\mathbf{6}^{+}\cdot PF_6^{-}$ is slightly more negative than that of $\mathbf{5}^{+}\cdot PF_6^{-}$. This might be attributable to the *tert*-butyl substituents at the 6-positions of the azulene rings, which stabilize the cationic state by their electron-donating nature. Meanwhile, the first oxidation wave of $\mathbf{5}^{+}\cdot PF_6^{-}$ is nearly identical to those of $\mathbf{6}^{+}\cdot PF_6^{-}$ to $\mathbf{10}^{+}\cdot PF_6^{-}$. These results show the lower degree of the contribution of substituents on the azulene ring to the oxidation potential of the ferrocene moiety.

To examine the color changes during the electrochemical reactions, spectral changes of cations $\mathbf{5}^{+}$, $\mathbf{6}^{+}$, and $\mathbf{9}^{+}$ were monitored by visible spectroscopy. Constant-current reduction was applied to solutions of $\mathbf{5}^{+}\cdot PF_6^{-}$, $\mathbf{6}^{+}\cdot PF_6^{-}$, and $\mathbf{9}^{+}\cdot PF_6^{-}$, with a platinum mesh as a working electrode and a wire counterelectrode, and visible spectra were measured in benzonitrile containing Et_4NClO_4 (0.1 M) as a supporting electrolyte at room temperature under electrochemical reduction conditions (see the Supporting Information).

The longest absorptions of $\mathbf{5}^{+}$, $\mathbf{6}^{+}$, and $\mathbf{9}^{+}$ gradually decreased, and the color of the solution changed adequately from green to yellow during the electrochemical reduction (Figure 5). However, reversible oxidation of the yellow-colored solution did not regenerate the spectrum of the corresponding starting compounds, as demonstrated in Figure 5 for $\mathbf{5}^{+}$, according to the reversibility of the redox process.

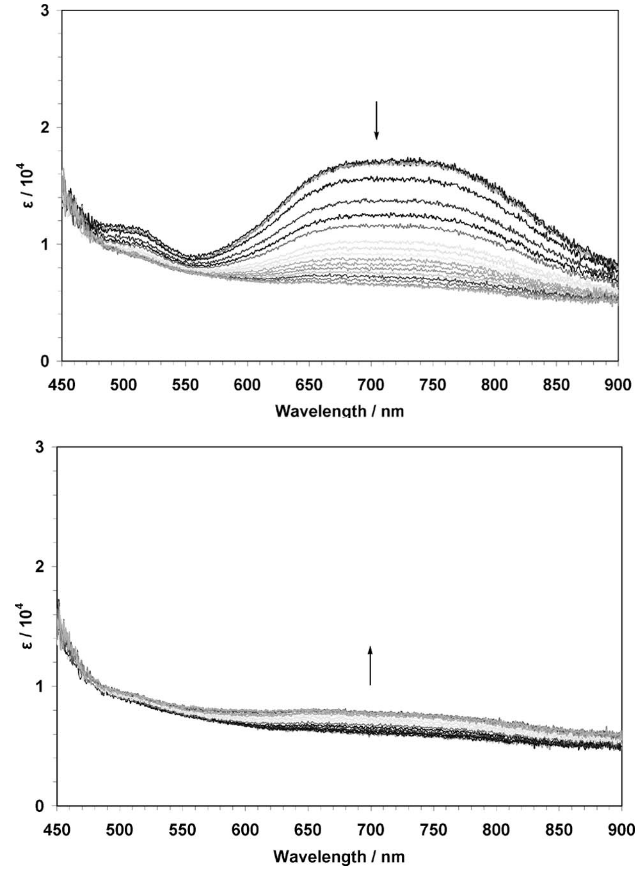

Figure 5. Continuous change in visible spectra of $\mathbf{5}^{+}\cdot PF_6^{-}$ in benzonitrile containing Et_4NClO_4 (0.1 M): constant-current electrochemical reduction (50 μA) at 30 sec intervals (upper) and reverse oxidation (bottom) of the reduced species (50 μA) at 30 sec intervals.

The non-reversibility of the color changes might be attributed to the instability of the reduced species. Although multistage reversible oxidation waves were observed in CV, compounds **5**$^+$, **6**$^+$, and **9**$^+$ did not exhibit reversible color changes, similar with electrochemical reduction. This irreversibility might be attributable to the instability of the cationic species under the measurement conditions.

Conclusions

Ferrocene derivatives have attracted interest due to their oxidation properties with lower potentials to form stabilized radical cationic states, that is, ferrocenium ions. Azulene derivatives with a ferrocenyl moiety are expected to show multiple-electron oxidation with reversible redox properties. We have synthesized novel ferrocene-substituted bis(3-methylthio-1-azulenyl)methyl cations **5**$^+$ and **6**$^+$ by the hydride abstraction reaction of the corresponding hydro derivatives **3** and **4** with DDQ. Analysis by CV and DPV showed that hydro derivatives **3** and **4** and cations **5**$^+$ and **6**$^+$ exhibit presumed amphoteric redox properties. Hydro derivatives **3** and **4** showed reversible three-stage oxidation waves, which might be attributed to the oxidation of ferrocene and two sulfur-substituted azulene moieties. Although cation **5**$^+$ displayed a reversible oxidation wave in CV, **6**$^+$ showed an irreversible oxidation wave. Significant color changes were observed during the electrochemical reduction of **5**$^+$, **6**$^+$, and **9**$^+$. However, the reverse oxidation of the reduced species did not regenerate the original color of the solutions of **5**$^+$, **6**$^+$, and **9**$^+$. These results might be attributed to the instability of the reduced species.

Experimental Section

General: Melting points were determined with a Yanagimoto MPS3 micro melting apparatus. Mass spectra were obtained with a Bruker APEX II instrument. IR and UV spectra were measured with a Shimadzu FTIR-8100M and a Hitachi U-3410 spectrophotometer, respectively. ^{1}H and ^{13}C NMR spectra were recorded with a JEOL GSX 400 (400 and 100 MHz) or a Bruker AVANCE400 (400 and 100 MHz). Voltammetry measurements were carried out with a BAS 100B/W electrochemical workstation equipped with Pt working and auxiliary electrodes and a reference electrode formed from Ag/AgNO$_3$ (0.1 M) in a tetrabutylammonium perchlorate (0.1 M)/acetonitrile solution. Elemental analyses were performed at the Research and Analytical Center for Giant Molecules, Graduate School of Science Tohoku University.

Bis(3-methylthio-1-azulenyl)ferrocenylmethane (3): A solution of **1** (524 mg, 3.01 mmol) and ferrocenecarbaldehyde (107 mg, 0.50 mmol) in glacial acetic acid was stirred at 50 °C for 24 h under an Ar atmosphere. The reaction mixture was diluted with CH_2Cl_2. The organic layer was washed with 5% aqueous $NaHCO_3$ and water, dried with $MgSO_4$, and concentrated under reduced pressure. The residue was purified by column chromatography on silica gel with CH_2Cl_2 to afford **3** (187 mg, 69%) as green crystals. M. p. 70.0–72.5 °C (AcOEt). HRMS (ESI): calcd. for $C_{33}H_{28}FeS_2^+$ [M]$^+$ 544.0976; found 544.0975. IR (KBr disk): $\tilde{\nu}_{max}$ = 3088 (w), 3018 (w), 2980 (m), 2914 (w), 1572 (s), 1497 (w), 1447 (w), 1396 (s), 1333 (w), 1298 (m), 1217 (w), 1105 (m), 1042 (w), 1024 (w), 1001 (m), 984 (w), 966 (w), 943 (w), 926 (w), 876 (w), 818 (m), 748 (m), 733 (s), 708 (w), 692 (w), 681 (w), 667 (w), 575 (w), 557 (w), 544 (w), 494 (m), 463 (w), 449 (w), 424 (w) cm^{-1}. UV/Vis (CH_2Cl_2): λ_{max} (log ε) = 242 (4.64), 287 (4.72), 298 sh (4.69), 320 sh (4.30), 372 (4.04), 617 (2.77), 652 sh (2.76) nm. ^{1}H NMR (400 MHz, $CDCl_3$): δ = 8.51 (d, J = 9.6 Hz, 2 H, 4-H), 8.37 (d, J = 9.6 Hz, 2 H, 8-H), 7.81 (s, 2 H, 2-H), 7.51 (t, J = 9.6 Hz, 2 H, 6-H), 7.11 (t, J = 9.6 Hz, 2 H, 5-H), 7.04 (t, J = 9.6 Hz, 2 H, 7-H), 6.34 (s, 1 H, CH), 4.15 (t, J = 2.0 Hz, 2 H, 3,4-H of Fc), 4.07 (t, J = 2.0 Hz, 2 H, 2,5-H of Fc), 3.89 (s, 5 H, Cp), 2.42 (s, 6 H, SCH_3) ppm. ^{13}C NMR (100 MHz, $CDCl_3$): δ = 140.14, 139.29, 138.28, 135.88, 135.20, 133.44, 133.16, 122.76, 122.49, 120.41, 94.42, 68.71, 68.63, 67.37, 36.44, 20.05 ppm. $C_{33}H_{28}FeS_2$ (544.55): calcd. C 72.79, H 5.18; found C 72.62, H 5.35.

Bis(3-methylthio-6-*tert*-butyl-1-azulenyl)ferrocenylmethane (4): A solution of **2** (690 mg, 3.00 mmol) and ferrocenecarbaldehyde (107 mg, 0.50 mmol) in glacial acetic acid was stirred at 50 °C for 24 h under an Ar atmosphere. The residue was diluted with CH_2Cl_2. The organic layer was washed with 5% aqueous $NaHCO_3$ and water, dried with $MgSO_4$, and concentrated under reduced pressure. The residue was purified by column chromatography on silica gel with CH_2Cl_2 to afford **4** (300 mg, 91%) as green crystals. M. p. 120.0–123.0 °C (CH_2Cl_2). HRMS (ESI): calcd. for $C_{41}H_{44}FeS_2^+$ [M]$^+$ 656.2234; found 656.2233. IR (KBr disk): $\tilde{\nu}_{max}$ = 3082 (w), 2963 (m), 2916 (w), 2868 (w), 1577 (s), 1495 (w), 1460 (w), 1408 (m), 1362 (w), 1339 (w), 1306 (w), 1252 (w), 1198 (w), 1182 (w), 1132 (w), 1107 (w), 1067 (w), 1042 (w), 1024 (w), 1001 (w), 964 (w), 926 (w), 837 (m), 820 (m), 756 (w), 741 (w), 675 (w), 617 (w), 496 (w), 448 (w) cm^{-1}. UV/Vis (CH_2Cl_2): λ_{max} (log ε) = 242 (4.60), 294 (4.80), 301 (4.80), 376 sh (4.02), 606 (2.81) nm. ^{1}H NMR (400 MHz, $CDCl_3$): δ = 8.45 (d, J = 10.4 Hz, 2 H, 8-H), 8.32 (d, J = 10.4 Hz, 2 H, 4-H), 7.75 (s, 2 H, 2-H), 7.30 (dd, J = 10.4, 1.6 Hz, 2 H, 7-H), 7.23 (dd, J = 10.4, 1.6 Hz, 2 H, 5-H), 6.30 (s, 1 H, CH), 4.12 (t, J = 2.0 Hz, 2 H, 3,4-H of Fc), 4.06 (t, J = 2.0 Hz, 2 H, 2,5-H of Fc), 3.91 (s, 5 H, Cp), 2.41 (s, 6 H, SCH_3), 1.41 (s, 18 H, *t*Bu) ppm. ^{13}C NMR (100 MHz, $CDCl_3$): δ = 162.49, 140.06, 138.65, 135.30, 134.59, 133.30, 133.23, 121.33, 121.21, 120.05, 95.24, 69.32, 69.16, 67.75, 38.99, 36.91, 32.29, 21.26 ppm. $C_{41}H_{44}FeS_2$ (656.77): calcd. C 74.98, H 6.75; found C 75.26, H 7.05.

Ferrocenyl Bis(3-methylthio-1-azulenyl)methylium Hexafluorophosphate (5$^+$·PF_6^-): DDQ (50 mg, 0.22 mmol) was added at room temperature to a solution of **3** (96 mg, 0.18 mmol) in CH_2Cl_2 (10 mL). After the solution was stirred at the same temperature for 30 min, a 60% HPF_6 (5 mL) solution was added to the mixture. After stirring at room temperature for an additional 15 min, water was added to the mixture. The resulting suspension was filtered with suction. The organic layer was separated, washed with water, dried with $MgSO_4$, and concentrated under reduced pressure. The residue was crystallized from CH_2Cl_2/Et_2O to give **5**$^+$·PF_6^- (117 mg, 96%) as a dark green powder. M. p. 160.0–165.0 °C (decomp.). HRMS (ESI): calcd. for $C_{33}H_{27}FeS_2^+$ [M – PF_6]$^+$ 543.0898; found 543.0896. IR (KBr disk): $\tilde{\nu}_{max}$ = 2910 (w), 1452 (s), 1420 (s), 1400 (s), 1381 (w), 1354 (m), 1324 (s), 1313 (s), 1302 (s), 1279 (s), 1189 (w), 1145 (w), 1108 (w), 1088 (w), 1060 (w), 1023 (w), 877 (m), 838 (s), 787 (w), 753 (m), 701 (w), 682 (w), 628 (w), 609 (w), 571 (w), 557 (m), 498 (w), 467 (w), 453 (w), 441 (w) cm^{-1}. UV/Vis (CH_3CN): λ_{max} (log ε) = 234 (4.58), 262 sh (4.52), 297 (4.54), 391 (4.31), 516 (3.83), 742 (4.21) nm. ^{1}H NMR (400 MHz, CD_3CN): δ = 8.69 (dd, J = 9.6, 1.6 Hz, 2 H, 4-H), 8.59 (s, 2 H, 2-H), 7.92–7.82 (m, 4 H, 5,6-H), 7.43 (dd, J = 9.6, 1.6 Hz, 2 H, 8-H), 7.26 (ddd, J = 9.6, 1.6, 1.6 Hz, 2 H, 7-H), 5.49 (dd, J = 2.0, 2.0 Hz, 2 H, 2,5-H of Fc), 5.22 (dd, J = 2.0, 2.0 Hz, 2 H, 3,4-H of Fc), 4.54 (s, 5 H, Cp), 2.82

(s, 6 H, SCH_3) ppm. ^{13}C NMR (100 MHz, CD_3CN): δ = 148.59, 148.47, 145.06, 141.65, 140.46, 140.06, 133.98, 133.51, 133.40, 87.24, 80.20, 78.43, 74.47, 17.90 ppm. $C_{33}H_{27}F_6FePS_2 \cdot 1/2H_2O$ (697.52): calcd. C 56.82, H 4.05; found C 57.00, H 4.16.

Ferrocenyl Bis(3-methylthio-6-*tert*-butyl-1-azulenyl)methylium Hexafluorophosphate ($6^+ \cdot PF_6^-$): DDQ (86 mg, 0.38 mmol) was added at room temperature to a solution of **4** (203 mg, 0.31 mmol) in CH_2Cl_2 (30 mL). After the solution was stirred at the same temperature for 30 min, a 60% HPF_6 (5 mL) solution was added to the mixture. After stirring at room temperature for an additional 15 min, water was added to the mixture. The resulting suspension was filtered with suction. The organic layer was separated, washed with water, dried with $MgSO_4$, and concentrated under reduced pressure. The residue was crystallized from CH_2Cl_2/Et_2O to give $\mathbf{6}^+ \cdot PF_6^-$ (230 mg, 93%) as a dark green powder. M. p. 198.0–203.0 °C (decomp.). HRMS (ESI): calcd. for $C_{41}H_{43}FeS_2^+$ [M – PF_6]$^+$ 655.2150; found 655.2142. IR (KBr disk): $\tilde{\nu}_{max}$ = 3115 (w), 2963 (m), 2922 (w), 2870 (w), 1576 (m), 1460 (s), 1429 (s), 1379 (m), 1356 (m), 1325 (s), 1294 (s), 1246 (m), 1219 (m), 1194 (m), 1109 (m), 1076 (m), 1061 (m), 1055 (m), 1018 (w), 974 (w), 924 (w), 839 (s), 775 (w), 743 (w), 708 (w), 669 (w), 617 (w), 594 (w), 557 (m), 500 (w), 482 (w) cm^{-1}. UV/Vis (CH_3CN): λ_{max} (log ε) = 234 (4.56), 264 (4.52), 302 (4.60), 391 (4.31), 493 (3.85), 738 (4.24) nm. ^1H NMR (400 MHz, CD_3CN): δ = 8.59 (d, J = 10.0 Hz, 2 H, 4-H), 8.48 (s, 2 H, 2-H), 8.04 (d, J = 10.0 Hz, 2 H, 8-H), 7.41 (d, J = 10.0 Hz, 2 H, 5-H), 7.34 (d, J = 10.0 Hz, 2 H, 7-H), 5.37 (br. s, 2 H, 3,4-H of Fc), 5.16 (br. s, 2 H, 2,5-H of Fc), 4.48 (s, 5 H, Cp), 2.78 (s, 6 H, SCH_3), 1.30 (s, 18 H, *t*Bu) ppm. ^{13}C NMR (100 MHz, CD_3CN): δ = 170.50, 147.72, 147.61, 140.80, 139.65, 138.84, 133.41, 133.27, 131.94, 86.49, 78.13, 79.1, 74.05, 40.43, 31.96, 18.10 ppm. $C_{41}H_{43}F_6FePS_2 \cdot 3/5CH_2Cl_2$ (851.68): calcd. C 58.67, H 5.23; found C 58.72, H 5.16.

Supporting Information (see footnote on the first page of this article): UV/Vis spectra and cyclic voltammograms of the reported compounds.

Acknowledgments

This work was partially supported by the Global Center of Excellence (GCOE) project, the International Center of Research & Education for Molecular Complex Chemistry, and the Ministry of Education, Culture, Sports, Science and Technology, Japan.

---

[1] a) P. L. Pauson, *Chem. Soc. Rev.* **1955**, *9*, 391–414; b) H. Nishihara, *Adv. Inorg. Chem.* **2002**, *53*, 41–86; c) D. R. van Staveren, N. M. Nolte, *Chem. Rev.* **2004**, *104*, 5931–5985; d) R. C. J. Atkinson, V. C. Gibson, N. Long, *J. Chem. Soc. Rev.* **2004**, *33*, 313–328; e) S. I. Kirin, H. B. Kraatz, N. M. Nolte, *Chem. Soc. Rev.* **2006**, *35*, 348–354.

[2] K.-P. Zeller, *Azulene in Methoden Org. Chem.* (*Houben-Weyl*), 4th ed. **1985**, vol. V, part 2c, pp. 127–418.

[3] a) M.-Å. Petersen, K. Kilså, A. Kadziola, M.-B. Nielsen, *Eur. J. Org. Chem.* **2007**, 1415–1418; b) M.-Å. Petersen, A.-S. Andersson, K. Kilså, M.-B. Nielsen, *Eur. J. Org. Chem.* **2009**, 1855–1858; c) M.-Å. Petersen, S.-L. Broman, A. Kadziola, K. Kilså, M.-B. Nielsen, *Eur. J. Org. Chem.* **2009**, 2733–2736.

[4] a) S. Ito, A. Nomura, N. Morita, C. Kabuto, H. Kobayashi, S. Maejima, K. Fujimori, M. Yasunami, *J. Org. Chem.* **2002**, *67*, 7295–7302; b) S. Ito, T. Okujima, N. Morita, *J. Chem. Soc. Perkin Trans. 1* **2002**, 1896–1905; c) S. Ito, H. Inabe, N. Morita, K. Ohta, T. Kitamura, K. Imafuku, *J. Am. Chem. Soc.* **2003**, *125*, 1669–1680; d) S. Ito, T. Kubo, N. Morita, T. Ikoma, S. Tero-Kubota, A. Tajiri, *J. Org. Chem.* **2003**, *68*, 9753–9762; e) S. Ito, H. Inabe, N. Morita, A. Tajiri, *Eur. J. Org. Chem.* **2004**, 1774–1780; f) S. Ito, T. Kubo, N. Morita, T. Ikoma, S. Tero-Kubota, J. Kawakami, A. Tajiri, *J. Org. Chem.* **2005**, *70*, 2285–2293; g) S. Ito, K. Akimoto, J. Kawakami, A. Tajiri, T. Shoji, H. Satake, N. Morita, *J. Org. Chem.* **2007**, *72*, 162–172; h) T. Shoji, S. Ito, K. Toyota, M. Yasunami, N. Morita, *Chem. Eur. J.* **2008**, *14*, 8398–8408; i) T. Shoji, S. Ito, K. Toyota, T. Iwamoto, M. Yasunami, N. Morita, *Eur. J. Org. Chem.* **2009**, 4316–4324; j) S. Ito, N. Morita, *Eur. J. Org. Chem.* **2009**, 4567–4579; k) S. Ito, T. Iida, J. Kawakami, T. Okujima, N. Morita, *Eur. J. Org. Chem.* **2009**, 5355–5364.

[5] S. Ito, N. Morita, T. Asao, *J. Org. Chem.* **1996**, *61*, 5077–5082.

[6] M.-R. Bryce, M.-A. Coffin, P.-J. Skabara, A.-J. Moore, A.-S. Batsanov, J.-A.-K. Howard, *Chem. Eur. J.* **2000**, *6*, 1955–1962.

[7] a) T. Shoji, S. Ito, K. Toyota, M. Yasunami, N. Morita, *Tetrahedron Lett.* **2007**, *48*, 4999–5002; b) T. Shoji, H. Higashi, S. Ito, K. Toyota, M. Yasunami, N. Morita, *Eur. J. Org. Chem.* **2008**, 1242–1252.

[8] J. Higashi, T. Shoji, S. Ito, K. Toyota, M. Yasunami, N. Morita, *Eur. J. Org. Chem.* **2008**, 5823–5831.

[9] T. Shoji, J. Higashi, S. Ito, K. Toyota, T. Iwamoto, N. Morita, *Eur. J. Org. Chem.* **2009**, 5948–5952.

Received: May 20, 2010
Published Online: September 2, 2010